Polyhedron 30 (2011) 114–122

Contents lists available at ScienceDirect

Polyhedron

journal homepage: www.elsevier.com/locate/poly

Synthesis, characterization, structures and cytotoxic activity of palladium(II) and platinum(II) complexes containing bis(2-pyridylmethyl)amine and saccharinate

Emel Guney [a], Veysel T. Yilmaz [a,*], Ferda Ari [b], Orhan Buyukgungor [c], Engin Ulukaya [d]

[a] Department of Chemistry, Faculty of Arts and Sciences, Uludag University, 16059 Bursa, Turkey
[b] Department of Biology, Faculty of Arts and Sciences, Uludag University, 16059 Bursa, Turkey
[c] Department of Physics, Faculty of Arts and Sciences, Ondokuz Mayis University, 55139 Samsun, Turkey
[d] Department of Medical Biochemistry, Faculty of Medicine, Uludag University, 16059 Bursa, Turkey

ARTICLE INFO

Article history:
Received 17 August 2010
Accepted 29 September 2010
Available online 7 October 2010

Keywords:
Saccharinate
Bis(2-pyridylmethyl)amine
Palladium(II)
Platinum(II)
Water cluster
Cytotoxic activity

ABSTRACT

New palladium(II) and platinum(II) complexes containing bis(2-pyridylmethyl)amine (bpma) and saccharinate (sac), [Pd(bpma)(sac)](sac)·2H_2O (**1**), [Pt(bpma)(sac)](sac)·2H_2O (**2**), [Pd(bpma)Cl](sac)·2H_2O (**3**) and [Pt(bpma)(sac)]Cl·1.5H_2O (**4**), were synthesized and characterized by elemental analysis, IR, NMR and TG-DTA. A single-crystal X-ray analysis of **3** and **4** proved a distorted square–planar geometry around the metal ions with one tridentate bpma ligand and one Cl or sac monoanion. The $[Pd(bpma)Cl]^+$ ions in **3** form dimers by intermolecular N–H···Cl and Pd···Pd interactions. The cations reside in the centers of a hydrogen-bonded honeycomb network formed by the uncoordinated sac ions and the lattice water molecules, while the cations of **4** are connected by N–H···Cl and OW–H···O hydrogen bonds into one-dimensional chains. Cyclic planar tetrameric and trimeric water clusters were observed in **3** and **4**, respectively. Cytotoxicity of **1**–**4** was tested against A549, C6 and CHO cells. Although **2** and **4** have no cytotoxicity, the best results were achieved for **1** and **3**. In particular, the cyctotoxic activity of **3** is comparable to cisplatin.

1. Introduction

Cisplatin, chemically named as *cis*-diamminedichloroplatinum(II), is an extensively used cytotoxic anti-cancer drug [1]. Despite its remarkable success, several side effects such as the dose-dependent nephrotoxicity, neuorotoxicity and emetogensis are major medical problems associated with this drug [2]. Carboplatin, *cis*-diammine(cyclobutane-1,1-dicarboxylate-*O*,*O*′)platinum(II), and oxaliplatin, (1*R*,2*R*)-cyclohexane-1,2-diamine](ethanedioato-*O*,*O*′)platinum(II), were approved as the second, and third platinum-based drug generations, respectively [3,4]. Both platinum(II) complexes met requirements of improving antitumor activity and reducing disadvantages of cisplatin to some extent [5]. Therefore, there are demands for the design and synthesis of new metal complexes with high antitumor activity and less side effects in this field. On the other hand, palladium(II) complexes show similar chemical and structural properties with those of platinum(II) complexes and are, therefore, expected to have antitumor activity. Recent studies demonstrate that some palladium(II) complexes exhibit a noticeable *in vitro* cytotoxic activity, comparable to standard platinum-based drugs, cisplatin, carboplatin and oxaliplatin [6].

The coordination chemistry of saccharin (sacH, also named 1,1-dioxo-1,2-benzothiazol-3-one or *o*-benzosulfimide) is interesting. SacH readily loses the amine hydrogen forming the saccharinate monoanion (sac) in solutions. Owing to the presence of the imino, carbonyl and sulfonyl donor sites, sac acts as a mono-, bi- or tridentate polyfunctional ligand and coordinates many transition metal ions, forming complexes from mononuclear species to coordination polymers [7]. Moreover, these donor sites together with the aromatic ring make sac as a good acceptor for non-covalent interactions such as hydrogen bonding and π···π stackings.

Our systematic studies have been directed to palladium(II) and platinum(II) complexes of sac, since palladium and platinum complexes of sac are rare and only a few complexes have been reported [8–12]. We have recently reported several palladium(II) and platinum(II) complexes of sac with 2,2′:6′,2″-terpyridine (terpy) [13], 2,2′-bipyridine (bpy) [14], 2,2′-dipyridylamine (dpya) [15], 2-aminomethyl (ampy) and -ethylpyridines (aepy) [16]. The cytotoxic activity of the palladium(II) and platinum(II) complexes with bpy and dpya was not tested due to their low solubility in common solvents. However, especially the palladium(II) complexes of terpy have demonstrated a distinct antitumor activity against a lung cancer cell line (A549) compared to cisplatin [17]. To the best of our knowledge, the structure of palladium(II) and platinum(II)-bis(2-pyridylmethyl)amine (bpma) complexes with sac and their cyctotoxic activity have not been reported. Herein, we report the

* Corresponding author.
E-mail address: vtyilmaz@uludag.edu.tr (V.T. Yilmaz).

0277-5387/$ - see front matter © 2010 Elsevier Ltd. All rights reserved.
doi:10.1016/j.poly.2010.09.037

synthesis, characterization, crystal structures of new palladium(II) and platinum(II) complexes of bpma with sac, namely [Pd(bpma)(sac)](sac)·2H_2O (**1**), [Pt(bpma)(sac)](sac)·2H_2O (**2**), [Pd(bpma)Cl](sac)·2H_2O (**3**) and [Pt(bpma)(sac)]Cl·1.5H_2O (**4**). *In vitro* cytotoxicity studies were performed using Chinese hamster ovary cell line (CHO), a human lung carcinoma cell line (A549), and a rat brain tumor (glioma) cell line (C6). The cytotoxic activity of new complexes **1**–**4** was compared to that of the standard chemotherapeutic drug, cisplatin.

2. Experimental

2.1. Materials and measurements

[M(bpma)Cl]Cl·H_2O (M = Pd^{II} or Pt^{II}) was prepared as described in the literature [18]. Other chemicals were purchased and used as received. Elemental analyses for C, H, and N were performed using a Costech elemental analyzer. UV–Vis spectra were measured on a Shimadzu 1700UV spectrophotometer using 1×10^{-5} M EtOH/water (1:1) solutions in the 200–800 nm range. IR spectra were recorded on a Thermo Nicolet 6700 FT-IR spectrophotometer as KBr pellets in the frequency range 4000–400 cm^{-1}. ^1H NMR and ^{13}C NMR spectra were recorded on a Varian Mercuryplus spectrometer. Excitation and emission spectra of 1×10^{-3} M EtOH/water solutions (1:1) were recorded at room temperature with a Varian Cary Eclipse spectrophotometer equipped with a Xe pulse lamp of 75 kW. Thermal analysis curves (TG and DTA) were obtained from a Seiko Exstar TG/DTA 6200 thermal analyzer in a flowing air atmosphere with a heating rate of 10 K min^{-1} using a sample size of 5–10 mg and platinum crucibles.

2.2. Synthesis of the palladium(II) and platinum(II) complexes

Complexes **1** and **2** were synthesized by the following method. Solid [M(bpma)Cl]Cl·H_2O (0.5 mmol) and solid $AgNO_3$ (1 mmol, 0.17 g) were added to water (200 ml) and set to reflux for 6 h. The precipitate of AgCl was removed by filtering through Celite paste to obtain a clear solution. The filtrate was concentrated to 25 ml and followed by the addition of Na(sac)·2H_2O (1 mmol, 0.24 g) and stirred at 60 °C for 30 min. Yellow polycrystalline solids of **1** and **2** were obtained after a day.

In order to prepare complexes of **3** and **4**, the solid [M(bpma)Cl]Cl·H_2O (0.5 mmol) was dissolved in 15 ml water and then, to this solution, a 5 ml aqueous solution of Na(sac)·2H_2O (0.5 mmol, 0.12 g) was added and stirred at 60 °C for 2 h. The resulting clear solution was allowed to stand at room temperature and yellow crystals of **3** and **4** were obtained after two days.

*[Pd(bpma)(sac)](sac)·2H_2O (**1**):* Yield 85%. M.p. 235–237 °C (decomp.). *Anal.* Calc. for $C_{26}H_{25}N_5O_8PdS_2$: C, 44.2; H, 3.6; N, 9.9. Found: C, 44.3; H, 3.8; N, 9.8%. ^1H NMR (400 MHz, DMSO-d_6): δ 8.70 (s, 1H, NH), 8.28–8.14 (td, 2H, $H^{4,4'}$), 8.14–8.00 (b, 2H, $H^{6,6'}$), 7.95–7.82 (m, 2H, $H^{5,5'}$), 7.82–7.69 (d, 2H, $H^{3,3'}$), 7.69–7.48 (m, 8H, H^{sac}), 5.45–4.80 (s, 2H, CH_2), 4.80–4.25 (s, 2H, CH_2). ^{13}C NMR (400 MHz, DMSO-d_6): δ 169.43, 168.48, 167.65, 151.36, 150.22, 146.62, 142.51, 142.24, 136.06, 135.09, 132.88, 132.31, 126.40, 126.09, 124.12, 123.91, 123.74, 121.82, 120.34, 59.67. (Solid KBr pellet): ν (cm^{-1}) 3527m, 3335mb, 3254sh, 3093m, 3069m, 2865w, 1681s, 1635vs, 1587m, 1479w, 1456w, 1330w, 1299vs, 1248vs, 1167vs, 1149vs, 1118s, 1055w, 1021w, 952m, 790m, 772w, 752m, 677m, 598s, 561w, 539m, 439w. UV–Vis (λ/nm) (ε/dm^3 mol^{-1} cm^{-1}): 264 (7585).

*[Pt(bpma)(sac)](sac)·2H_2O (**2**):* Yield 82%. M.p. 245–250 °C (decomp.). *Anal.* Calc. for $C_{26}H_{25}N_5O_8PtS_2$: C, 39.3; H, 3.2; N, 8.8. Found: C, 39.3; H, 3.3; N, 8.9%. ^1H NMR (400 MHz, DMSO-d_6): δ 8.90 (s, 1H, NH), 8.56–8.38 (d, 2H, $H^{6,6'}$), 8.35–8.15 (td, 2H, $H^{4,4'}$), 7.97–7.85 (m, 2H, $H^{5,5'}$), 7.85–7.72 (d, 2H, $H^{3,3'}$), 7.72–7.43 (m, 8H, H^{sac}), 5.18–4.98 (m, 2H, CH_2), 4.86–4.58 (m, 2H, CH_2). ^{13}C NMR (400 MHz, DMSO-d_6): δ 167.72, 166.93, 166.74, 150.42, 150.12, 142.13, 140.87, 140.30, 136.03, 135.01, 131.58, 131.03, 125.30, 125.12, 124.01, 122.88, 122.51, 120.51, 119.13, 58.66. (Solid KBr pellet): ν (cm^{-1}) 3530m, 3381mb, 3258sh, 3089m, 3069m, 2862w, 1686vs, 1635vs, 1585m, 1479w, 1455m, 1331m, 1303vs, 1248vs, 1169vs, 1149vs, 1118s, 1056m, 1025w, 952m, 790m, 752m, 678m, 598s, 564m, 536m, 449w. UV–Vis (λ/nm) (ε/dm^3 mol^{-1} cm^{-1}): 270 (19 217).

*[Pd(bpma)Cl](sac)·2H_2O (**3**):* Yield 92%. M.p. 235–240 °C. *Anal.* Calc. for $C_{19}H_{21}ClN_4O_5PdS$: C, 40.8; H, 3.8; N, 10.0. Found: C, 40.6; H, 4.1; N, 9.8%. ^1H NMR (400 MHz, DMSO-d_6): δ 9.05 (s, 1H, NH), 8.66–8.51 (d, 2H, $H^{6,6'}$), 8.26–8.08 (td, 2H, $H^{4,4'}$), 7.81–7.70 (d, 2H, $H^{3,3'}$), 7.69–7.51 (m, 6H, $H^{5,5'}$ and H^{sac}), 5.33–4.68 (s, 2H, CH_2), 4.68–4.12 (s, 2H, CH_2). ^{13}C NMR (400 MHz, DMSO-d_6): δ 168.30, 166.61, 150.41, 145.73, 141.62, 135.26, 132.01, 131.43, 125.33, 123.14, 122.94, 119.56, 58.72. (Solid KBr pellet): ν (cm^{-1}) 3396mb, 3136m, 3097m, 2966w, 2934w, 2874w, 1640vs, 1609m, 1584m, 1479w, 1442m, 1330w, 1254vs, 1168m, 1136vs, 1054w, 1010w, 955m, 775s, 722w, 684m, 604m, 549m, 528m, 489w, 439w. UV–Vis (λ/nm) (ε/dm^3 mol^{-1} cm^{-1}): 263 (14 119).

*[Pt(bpma)(sac)]Cl·1.5H_2O (**4**):* Yield 90%. M.p. 230–240 °C (decomp.). *Anal.* Calc. for $C_{19}H_{20}ClN_4O_{4.5}PtS$: C, 35.7; H, 3.2; N, 8.8. Found: C, 35.8; H, 3.3; N, 8.7%. ^1H NMR (400 MHz, DMSO-d_6): δ 8.93–8.78 (d, 2H, $H^{6,6'}$), 8.69 (s, 1H, NH), 8.33–8.16 (td, 2H, $H^{4,4'}$), 7.86–7.72 (d, 2H, $H^{3,3'}$), 7.72–7.51 (m, 6H, $H^{5,5'}$ and H^{sac}), 5.03–4.86 (q, 2H, CH_2), 4.75–4.53 (d, d, 2H, CH_2). ^{13}C NMR (400 MHz, DMSO-d_6): δ 167.85, 166.95, 148.81, 145.23, 140.88, 134.72, 131.56, 131.00, 125.14, 122.87, 122.48, 120.00, 58.82. (Solid KBr pellet): ν (cm^{-1}) 3373mb, 3130m, 3101m, 2974w, 2934w, 2874w, 1641vs, 1613m, 1584m, 1482w, 1442m, 1330w, 1254vs, 1168m, 1138vs, 1054w, 1016w, 955m, 777s, 724w, 685m, 605m, 550m, 528m, 494w, 450w. UV–Vis (λ/nm) (ε/dm^3 mol^{-1} cm^{-1}): 273 (23 056).

2.3. X-ray crystallography

The intensity data of the complexes **3** and **4** were collected using a STOE IPDS 2 diffractometer with graphite-monochromated

Table 1
Crystallographic data and structure refinement for **3** and **4**.

Complex	**3**	**4**
Formula	$C_{19}H_{21}ClN_4O_5PdS$	$C_{19}H_{20}ClN_4O_{4.5}PtS$
M	559.31	638.99
T (K)	296(2)	296(2)
λ (Å)	0.71073	0.71073
Crystal system	monoclinic	monoclinic
Space group	$P2_1/c$	$C2/c$
a (Å)	7.7947(4)	22.8136(12)
b (Å)	23.4307(16)	7.4613(3)
c (Å)	14.1668(8)	26.8694(11)
β (°)	123.322(3)	116.580(3)
V (Å^3)	2162.0(2)	4090.3(3)
Z	4	4
D_{calcd} (g cm^{-3})	1.719	2.075
μ (mm^{-1})	1.118	7.132
F(0 0 0)	1128	2472
θ range (°)	1.93–26.50	1.69–25.64
Index range	$-9 \leqslant h \leqslant 9$, $-29 \leqslant k \leqslant 26$, $-17 \leqslant l \leqslant 17$	$-25 \leqslant h \leqslant 27$, $-9 \leqslant k \leqslant 9$, $-32 \leqslant l \leqslant 32$
Reflections collected	13122	17137
Data/parameters	4453/292	3853/286
Goodness-of-fit (GOF) on F^2	1.013	1.140
R_1 [$I > 2\sigma$]	0.0426	0.0393
wR_2	0.1138	0.0898

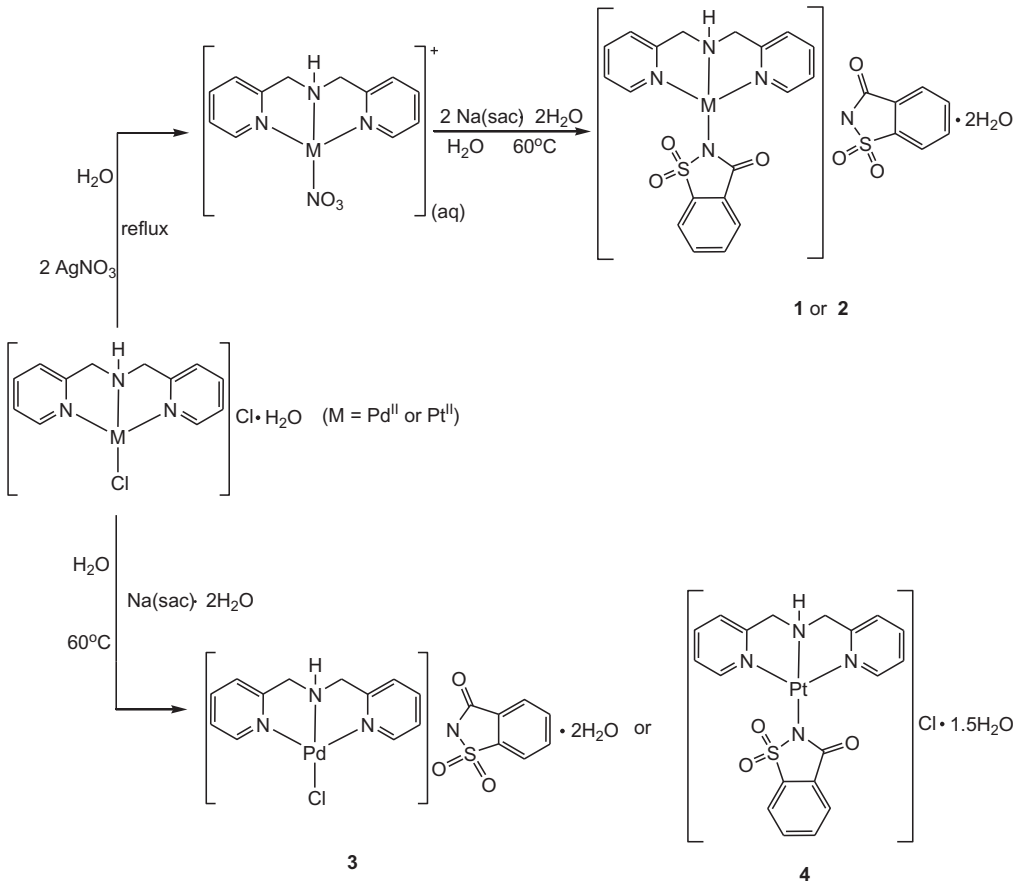

Scheme 1. Synthesis of complexes **1**–**4**.

Table 2
Selected FT-IR spectral data for **1**–**4**[a].

Assignment	1	2	3	4
ν(OH)	3527m, 3335mb	3530m, 3381mb	3396mb	3373mb
ν(NH)	3254sh	3258sh	3136m	3130m
ν(CH)	3093m–2865w	3089m–2862w	3097m–2874w	3101m–2874w
ν(CO)	1681s, 1635vs	1686vs, 1635vs	1640vs	1641vs
ν_s(CNS)	1330w	1331m	1330w	1330w
ν_{as}(SO_2)	1299vs, 1248vs	1303vs, 1248vs	1254vs	1254vs
ν_s(SO_2)	1167vs, 1149vs	1169vs, 1149vs	1168m, 1136vs	1168m, 1138vs
ν_{as}(CNS)	952m	952m	955m	955m

[a] Frequencies in cm^{-1}. b = broad; m = medium; w = weak; vw = very weak; vs = very strong; s = strong; sh = shoulder.

Mo Kα radiation (λ = 0.71073 Å). The structures were solved by direct methods and refined on F^2 with the SHELX-97 program [19]. All non-hydrogen atoms were found from the difference Fourier map and refined anisotropically. Hydrogen atoms bonded to C and N atoms were refined using a riding model, with C–H = 0.93–0.97 Å and N–H = 0.91 Å. The constraint $U_{iso}(H) = 1.2U_{eq}$(C and N) or $1.5U_{eq}$(methyl C) was applied. The water hydrogen atoms are refined freely. The details of data collection, refinement and crystallographic data are summarized in Table 1.

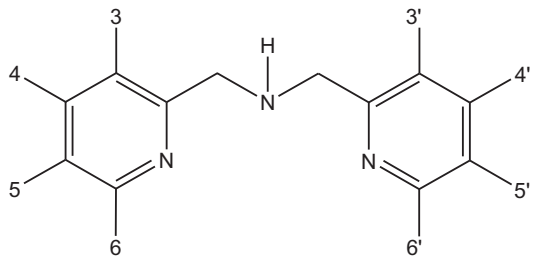

Scheme 2. Numbering of the protons of bpma.

2.4. In vitro cytotoxicity studies

Cisplatin was obtained from Sigma (St. Louis, MO, USA). Stock concentrations of the complexes **1**–**4** were prepared in culture medium, while that of cisplatin in DMSO, and the final concentrations were prepared in culture medium in six different concentrations ranging from 3.25 to 100 μM were used.

The human lung cell cancer cell line A549, Chinese hamster ovary cell line CHO, and C6 glioma cell line were cultured in Ham's F-12 supplemented with penicillin G (100 U/ml), streptomycin (100 μg/ml), L-glutamine, and 10% fetal calf serum at 37 °C in a humidified atmosphere containing 5% CO_2.

The 3-(4,5-dimethylthiazol-2-yl)-2,5-diphenyltetrazoliumbromide (MTT) cell viability assay was performed as previously described [20]. For the MTT assay, the cells were seeded in 200 μl culture medium in triplicates at a density of 5×10^3 cells per well in a 96-well plate. Cells were treated with different concentration of each complex and cisplatin for 72 h. For minimum viability control, cells were incubated with 1 mM H_2O_2 (positive control for cell death). Untreated cells grown in culture medium were used for the maximum viability control (negative control for cell death). MTT was supplied as a stock solution (5 mg/ml PBS, pH 7.2) and sterile-filtered. At the end of the treatment period, 20 μl of MTT solution was added to each well and then, after another 4 h at 37 °C,

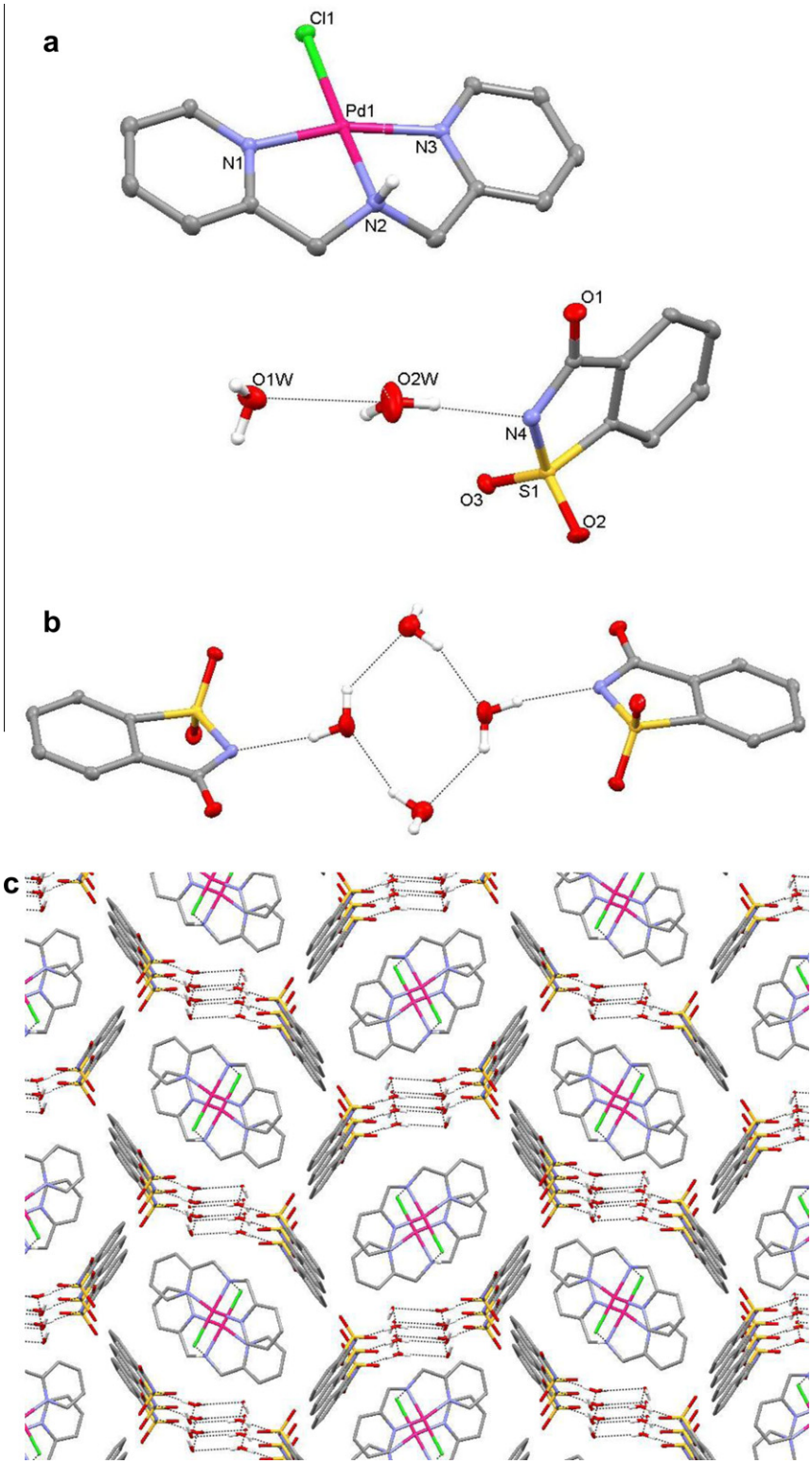

Fig. 1. (a) Molecular structure of [Pd(bpma)Cl](sac)·2H_2O (**3**). C–H hydrogen atoms were omitted for clarity. (b) A view of the tetrameric water cluster in **3**. (c) Two-dimensional network of **3**, viewed down the *a* axis, showing $[Pd(bpma)Cl]^+$ ions in a honeycomb structure formed by the hydrogen bonded sac ions and water molecules.

100 μl of solubilizing buffer (10% SDS dissolved in 0.01 N HCl) was added to each well. After overnight incubation, the absorbance was determined by an ELISA plate reader (FLASH Scan S12, Analytik Jena, Germany) at 570 nm as a read-out for cell viability. The cytotoxicity is mainly determined by the IC_{50} value of each metal complex. The IC_{50} values are drug concentrations that inhibit cell growth for 50% with respect to control.

3. Results and discussion

3.1. Synthesis

Complexes **1** and **2** are prepared by the reaction of the $[M(bpma)Cl]^+$ ion (M = Pt^{II} or Pd^{II}) with the stoichiometric amount of Na(sac) after removal of the chlorides in $[M(bpma)Cl]Cl{\cdot}H_2O$ by using $AgNO_3$, while **3** and **4** are synthesized by the direct reaction of $[M(bpma)Cl]Cl{\cdot}H_2O$ with Na(sac) in solution (Scheme 1). Complexes **1** and **2** can also be prepared using the similar method of **3** and **4**, but the purity and yield of these compounds were found to be low. Complexes **1** and **2** are formulated as $[M(bpma)(sac)](sac){\cdot}2H_2O$, in which the metal ions are coordinated by a sac ligand and a bpma ligand, while one sac anion remains as a counterion. The structures of **3** and **4** differ due to the coordination of Cl^- and sac anions. In $[Pd(bpma)Cl](sac){\cdot}2H_2O$ (**3**), the Cl^- anion is in the coordination sphere and sac is a counterion, whereas in $[Pt(bpma)(sac)]Cl{\cdot}1.5H_2O$ (**4**) vice versa. All complexes were crystallized, but only **3** and **4** yielded single crystals suitable for X-ray diffraction. All complexes are air-stable, water-soluble and obtained in high yields (over 80%).

3.2. Spectroscopic characterization

The electronic spectra were measured using 1×10^{-5} M EtOH/water (1:1) solutions of the ligands and their complexes. The free bpma and Na(sac) display single absorption bands in the UV region centered at 260 and 269 nm, respectively. These absorption bands are attributed to the π–π^* transitions. The spectra of **1**–**4** display broad bands in the range of 264–273 nm, including transitions of both bpma and sac ligands. The absence of shifts between the absorption bands of the free ligands and the complexes clearly indicates that the spectra of the metal complexes are dominated mainly by ligand-based transitions.

The selected IR bands of the complexes are listed in Table 2. The IR spectra show one or two broad bands centered over 3340 nm, due to the ν(OH) vibrations of the lattice water molecules, while the single bands in the frequency range 3090–3140 cm^{-1} are attributed to the NH stretching of the bpma ligand, which significantly shifted to the low frequency region compared to that of the free bpma ligand (3293 cm^{-1}). The sac moiety is characterized by the IR bands of the carbonyl and sulfonyl groups. Complexes **1** and **2** exhibit two sharp bands centered at ca. 1685 and 1635 cm^{-1} due to the absorption of the carbonyl groups of both coordinated and uncoordinated sac anions. But in the spectra of **3** and **4**, the carbonyl groups appeared as sharp bands at around 1640 cm^{-1}. The splitting of the carbonyl bands in the spectra of **1** and **2** indicates the presence of two different sac anions as observed in the IR spectra of the palladium(II) and platinum(II) complexes of terpy with sac [13]. The antisymmetric (ν_{as}) and symmetric (ν_s) stretchings of the SO_2 group are observed as two strong IR bands, which appeared two bands in **1** and **2** at ca. 1300–1248 and 1170–1149 cm^{-1}, respectively, while in **3** and **4** appeared as a single band at 1254 and 1138 cm^{-1}, respectively. The ν_s and ν_{as} stretching modes of the CNS moiety of the sac ligands appear at ca. 1330 and 955 cm^{-1}, respectively.

The signals in the ^{1}H NMR spectra of complexes **1**–**4** are assigned according to the numbering diagram in Scheme 2. The spectra of the metal complexes are similar. The NH proton appear as a singlet in the range δ 9.05–8.69 ppm. The pyridine protons appear as four signals between 8.93 and 7.51 ppm, while the protons of sac are observed as a multiplet in the range δ 7.72–7.43 ppm. In the spectra of **3** and **4**, the signals of the $H^{3,3'}$ atom of the bpma ligand overlap with those of sac. The proton resonances of the CH_2 group of bpma appear as a broad doublet at δ 5.00 and 4.50 ppm, whereas they are observed as a singlet in the spectra of the reported mixed-ligand bpma complexes of platinum(II) [18]. Contrary to the palladium(II) and platinum(II) complexes of terpy with sac [13], the proton resonances of the coordinated and uncoordinated sac rings occur in the same frequency range. The signals of ^{13}C NMR are consistent with the number of the C atoms in the structures of the metal complexes.

3.3. Description of crystal structures

The molecular structure of complex **3** is shown in Fig. 1a. Selected bond distances and angles are listed in Table 3. Complex **3** consists of a $[Pd(bpma)Cl]^+$ cation, a sac anion and two lattice water molecules. The palladium(II) ion has a distorted square–planar coordination arrangement with a tridentate bpma ligand and a Cl^- ligand. The distortion in the coordination geometry is mainly due to conformation of the bpma ligand, which gives rise to narrowing the angles. The structure of the cation is identical to the chloride salt, $[Pd(bpma)Cl]Cl{\cdot}H_2O$ [21]. The Pd–N bond distances are similar ranging from 2.007(4) to 2.014(3) Å, while the Pd–Cl bond distance is 2.296(1) Å. These bond distances are typical for the palladium(II) complexes containing bpma or ligands with the bpma moiety [21–26]. The two py rings are close to planarity with an angle of 4.20°.

Table 3
Selected bond lengths [Å], angles [°] and hydrogen bonding parameters for **3** and **4**[a].

	3	4
M1–N1	2.014(3)	2.026(6)
M1–N2	2.007(4)	1.995(7)
M1–N3	2.012(4)	2.010(6)
M1–N4	–	2.038(6)
M1–Cl1	2.296(1)	–
N1–M1–N2	82.80(15)	82.6(2)
N1–M1–N3	165.70(13)	165.7(3)
N1–M1–N4	–	97.0(2)
N2–M1–N3	83.84(15)	83.6(2)
N2–M1–N4	–	178.9(2)
N3–M1–N4	–	96.7(2)
N1–M1–Cl1	96.73(10)	–
N2–M1–Cl1	175.42(11)	–
N3–M1–Cl1	96.99(9)	–

Hydrogen bonds

D–H···A	D–H (Å)	H···A (Å)	D···A (Å)	D–H···A (°)
3				
O1W–H1W···O2W^{i}	0.84(7)	1.96(5)	2.753(8)	157(11)
O1W–H11W···O3^{ii}	0.83(9)	2.31(9)	3.128(5)	168(8)
O2W–H2W···O1W^{iii}	0.83(15)	2.25(10)	2.856(10)	130(11)
O2W–H21W···N4^{ii}	0.83(11)	2.07(11)	2.885(6)	170(12)
N2–H2A···Cl1^{iv}	0.91	2.45	3.274(4)	151
4				
N2–H2A···Cl1	0.91	2.29	3.132(7)	155
O2W–H3W···Cl1	0.83(14)	2.54(10)	3.363(12)	170(15)
O1W–H1W···O3^{v}	0.84(14)	2.44(10)	3.206(16)	152(20)
O1W–H2W···Cl1^{vi}	0.83(16)	2.60(8)	3.380(14)	155(18)

[a] Symmetry codes: (i) $x+1, y, z$; (ii) $-x+1, y+1/2, -z+3/2$; (iii) $-x+1, -y+2, -z+1$; (iv) $-x+2, -y+1, -z+1$; (v) $x+1/2, y-1/2, z$; (vi) $-x+3/2, y+1/2, -z+3/2$.

In the solid state, complex **3** exhibits an interesting hydrogen bonding scheme as listed in Table 3. The $[Pd(bpma)Cl]^+$ cations are doubly bridged into dimeric units by N–H···Cl hydrogen bonds, and orientation is head-to-tail. Moreover, the dimeric units are reinforced by a Pd–Pd interaction with a distance of 3.475 Å. In addition, the lattice water molecules O1W and O2W are connected with two symmetrically related water molecules by O1W–H1W···O2W and O2W–H2W···O1W hydrogen bonding interactions, leading to a D_{2h}-symmetric cyclic $(H_2O)_4$ water cluster (Fig 1b). The water tetramer is similar to that observed in $[Cd_3(pbtz)_3(DMF)_4(H_2O)_2]\cdot(DMF)_4(H_2O)_4$, where 2H-pbtz is 5,5′-(1,4-phenylene)bis(1H-tetrazole) [27]. The four co-crystallized water molecules are also involved in hydrogen bonds with the adjacent sac ions to form the honeycomb structure in the crystallographic *bc* plane as illustrated in Fig 1c. The $[Pd(bpma)Cl]^+$ cations occupy the centers of the honeycomb network and form weak C–H···O hydrogen bonds with the carbonyl and sulfonyl O atoms of the uncoordinated sac anions.

The molecular structure of **4** is shown in Fig. 2a and selected bond distances and angles are listed in Table 3. The complex is composed of $[Pt(bpma)(sac)]^+$ cation, a chloride counterion and lattice water molecules. The platinum(II) ion is coordinated by a tridentate bpma ligand and a sac ligand, forming a distorted square–planar geometry of PtN_4. In contrast to **3**, the sac anion

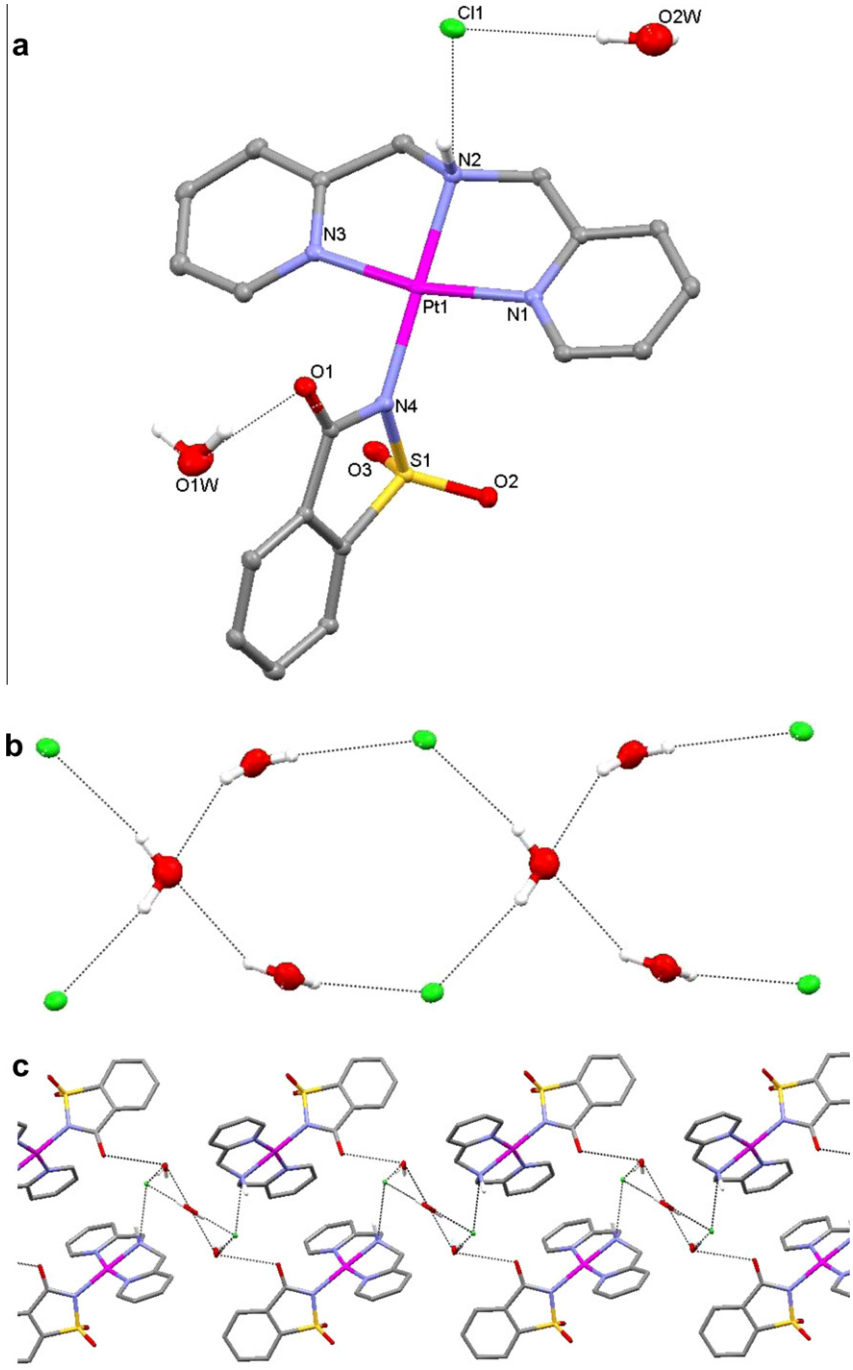

Fig. 2. (a) Molecular structure of $[Pt(bpma)(sac)]Cl\cdot1.5H_2O$ (**4**). C–H hydrogen atoms were omitted for clarity. (b) A view of the trimeric water cluster in **4**. (c) A view of one-dimensional hydrogen-bonded chain in **4**.

coordinates the metal and the chloride anion remains outside the coordination sphere as a counterion. In order to reduce steric hindrance, the sac ligand tends to be oriented perpendicularly to the coordination plane with a dihedral angle of 79.67°. Both py rings of bpma are almost co-planar as in **3**. The Pt–N(bpma) bond lengths are typical of those found in platinum(II) complexes containing the dpya ligand [18,28], while the Pt–N(sac) bond distance of 2.038(6) Å is within the expected range of platinum(II)–sac complexes [1.990(15)–2.064(6) Å] [10,11,13–15].

In the crystal lattice of **4**, two crystallographically independent water molecules (O1W and O2W) are observed and they are associated by hydrogen bonds to form a water trimer. The water trimers form hydrogen bonds with the neighboring chloride anions forming an irregular hexagonal ring (Fig 2b). The water molecules and chloride anions are further connected to the $[Pt(bpma)(sac)]^+$ cations by strong N–H···Cl and OW–H···Cl hydrogen bonds, leading to one-dimensional chain running along the *b* axis (Fig. 2c). The hydrogen-bonded chains are extended into a three-dimensional network by weak π(bpma)···π(bpma) stacking interactions where the shortest Cg···Cg contact is 3.795 Å (Cg is the center of gravity of the ring).

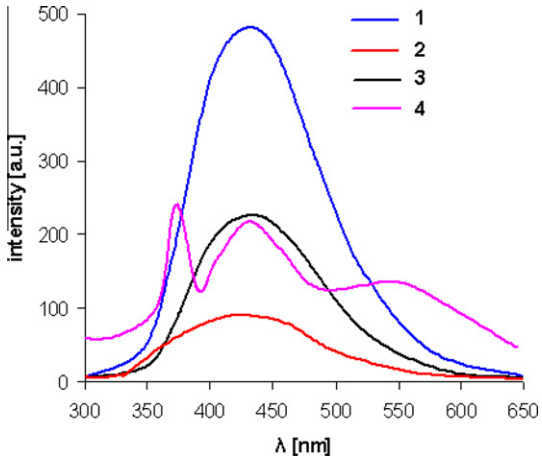

Fig. 3. Emission spectra of **1**–**4** in EtOH/water solutions (1:1) at room temperature.

3.4. Photoluminescence

The room temperature emission spectra of complexes **1**–**4** are presented in Fig. 3. The ligands and their metal complexes are weakly fluorescent upon excitation at their absorption wavelengths. However, when bpma and sac are excited at 357 and 285 nm, respectively, they moderately fluoresce at ca. 430 nm. On the other hand, complexes **1**–**3** have a single emission band, being emissive at 432 nm when excited at ca. 300 nm. Complex **1** showed maximum emission intensity. The resemblance of the emission spectra of **1**–**3** with those of the ligands indicates that the fluorescence of the complexes is due to the ligand-based π–π* transitions at the excited state. Since both sac and bpma ligands are emissive at the similar wavelength (ca. 430 nm), the transitions in the metal complexes may be originated from both ligands. Upon excitation at 335 nm, complex **4** exhibits three emission bands at 374, 432 and 553 nm. The higher energy bands may be attributed to the π–π* transitions, while the band at 553 nm can tentatively assigned to a metal-to-ligand charge transfer (MLCT) at the excited state [29,30].

3.5. Thermal behavior

The thermal stability and thermal decomposition behavior of complexes **1**–**4** were studied by a simultaneous TG/DTA analysis in the atmosphere of air. The thermoanalytical data are presented in Table 4. In general, the palladium complexes (**1** and **3**) decompose in four stages, while the platinum complexes (**2** and **4**) in

Table 5
IC_{50} values of complexes **1**–**4** and cisplatin.

Complex	IC_{50} (μM)		
	A546[a]	C6[b]	CHO[c]
[Pd(bpma)(sac)](sac)·2H_2O (**1**)	43	65	21
[Pt(bpma)(sac)](sac)·2H_2O (**2**)	>100	>100	>100
[Pd(bpma)Cl](sac)·2H_2O (**3**)	23	43	12
[Pt(bpma)(sac)]Cl·1.5H_2O (**4**)	>100	>100	>100
Cisplatin	20	14	11

[a] Human lung cancer cell.
[b] Glioma cell.
[c] Normal cell.

Table 4
TG/DTA data for **1**–**4**.

	Stage	Temperature range (°C)	DTA_{max} (°C)[a]	Mass loss (%)[b]	Solid residue
1	1	30–111	68 (+)	5.3 (5.1)	[Pd(bpma)(sac)](sac)
	2	200–380	236 (−), 253 (−)	42.5 (77.0)	–
	3	380–573	567 (−)	34.6 (77.0)	PdO
	4	810–878	817 (+)	1.6 (2.2)	Pd
				Total: 84.0 (84.9)	
2	1	35–113	75 (+)	4.5 (4.5)	[Pt(bpma)(sac)](sac)
	2	221–385	247 (−)	23.2 (25.1)	$[Pt(sac)_2]$
	3	385–505	501 (−)	46.8 (45.9)	Pt
				Total: 74.5 (75.5)	
3	1	37–127	87 (+)	4.7 (6.4)	[Pd(bpma)Cl](sac)
	2	222–380	235(+), 277 (−)	36.5 (35.6)	[PdCl(sac)]
	3	380–647	590 (−)	33.9 (32.6)	PdO
	4	815–849	834 (+)	3.4 (2.9)	Pd
				Total: 78.5 (77.5)	
4	1	45–94	79 (+)	5.6 (4.2)	[Pt(bpma)(sac)]Cl
	2	233–372	252 (−)	26.0 (65.3)	–
	3	372–514	504 (−)	39.1 (65.3)	Pt
				Total: 70.7 (69.5)	

[a] (+) and (−) donate endothermic and exothermic processes.
[b] Calculated values are given in parentheses.

three stages. All complexes dehydrate in the range of 30–115 °C and the mass losses are consistent with the water content of the metal complexes. The anhydrous complexes are stable up to 230 °C and the exothermic elimination of bpma begins over this temperature. It is followed by the highly exothermic decomposition of the sac moiety. In case of complexes **1** and **4**, the decomposition processes of bpma and sac overlap and it is impossible to estimate the mass losses associated with the individual ligands. The end product for the palladium(II) complexes is PdO, which decomposes to metallic Pd over ca. 800 °C, while the platinum(II) complexes produce metallic Pt at ca. 510 °C. The overall mass losses determined by the TG analyses agree well with those calculated to PdO or Pt as the final product of thermal decomposition (Table 4).

3.6. Cytotoxic activity

The cytotoxic effects of complexes **1**–**4** were assessed by the MTT assay. A549, CHO and C6 cells were treated for 72 h with increasing doses of complexes **1**–**4** and cisplatin. Viability was assessed and then the IC_{50} values were calculated (Table 5). The complexes yielded interesting results. Based on the IC_{50} values, complex **3** was found to be the most potent/cytotoxic one. In addition, complexes **2** and **4** resulted in no cytotoxic effect on the cell lines used (Fig. 4). This may imply that they have either no biologically active in cells, or not being taken up by cells, or pumped out by cells through the multidrug resistance proteins. However, palladium complexes are considered that they might always be promising in medicine as anti-cancer agents and encourage further studies in the field [6]. Various cells were treated with a large number of palladium complexes, but A549 and C6 cells have received less attention [6]. In this work, we have selected these cells in order to explore their behavior towards the new complexes. The results of the present study clearly show that complex **3** was especially potent in inducing cell death in the cell lines used, especially being comparable with cisplatin in the case of A549 cells. Regarding the palladium complexes in the literature, IC_{50} values seem to vary in a broad range from 0.5 [31] to 2500 μM [32]. IC_{50} values for **3** with different cell lines in our study ranged from 12 to 43 μM, which are clinically achievable doses. In another study in which two different palladium complexes, $[Pd(dmnp)_2Cl_2]$ and $[Pd_2(dmnp)_2Cl_4]$ (dmnp = 2,6-dimethyl-4-nitro-pyridine), used in A549 cells [33], it was reported that the corresponding IC_{50} values ranged from 8.4 to 21.3 μg/ml (estimated as 17.4 to 32.3 μM). These values are in good agreement with our result of complex **3** that was 23 μM for the same cell line. On the other hand, extremely low IC_{50} values (0.5 and 0.75 μM) were reported for C6 cells treated with the palladium(II) complexes [Pd(C2-dmba)(N_3)(dppp)] and [Pd(C2-*N*-dmba)(*cis*-dppet)](N_3) (dmba = N,N-dimethylbenzylamine, dppp = 1,3-bis(diphenylphosphino)propane and N_3^- = azide) [31].

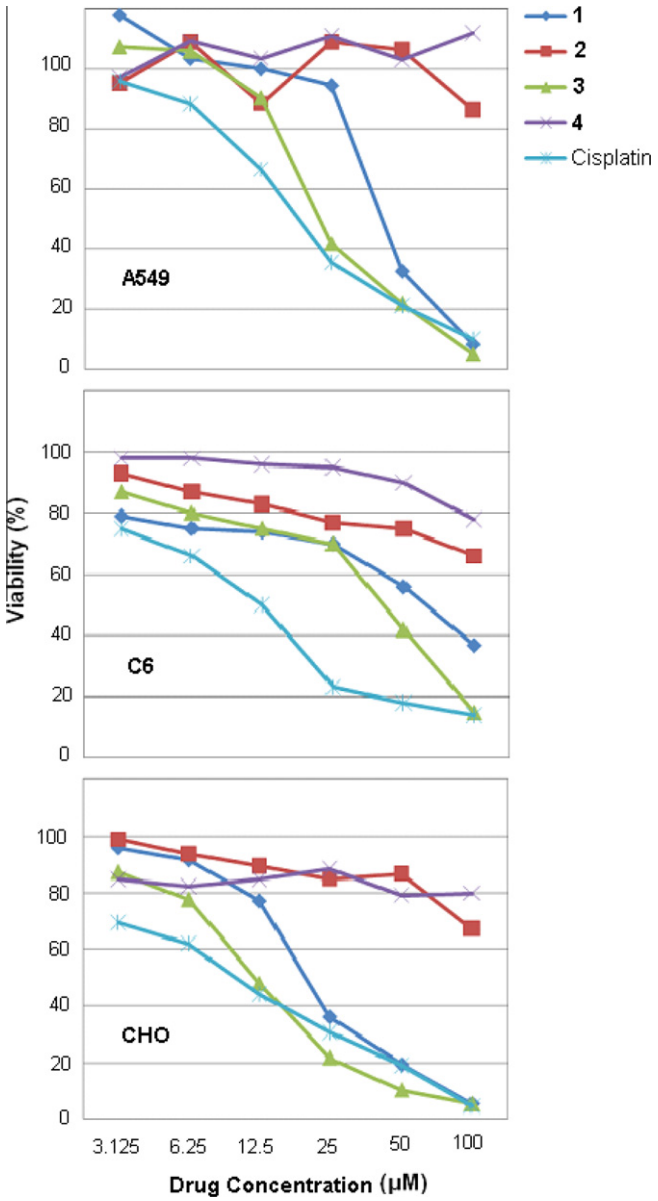

Fig. 4. Cytotoxicity of complexes **1**–**4** and cisplatin against A549, C6 and CHO cells.

4. Conclusions

A series of novel palladium(II) and platinum(II) complexes of bpma with sac have been synthesized and characterized by elemental analysis, FT-IR and NMR spectroscopy. Two representative complexes, $[Pd(bpma)Cl](sac)\cdot 2H_2O$ (**3**) and $[Pt(bpma)(sac)]Cl\cdot 1.5H_2O$ (**4**), were subjected to X-ray crystallographic analysis. The crystal structures exhibit that the palladium(II) and platinum(II) ions achieve a typical square planar arrangement. The complexes show photoluminescence in solution. The cytotoxicity of the complexes was evaluated in the normal cell line (CHO) and two cancer cell lines (A549 and C6). Significant differences have been found in the *in vitro* studies of the palladium(II) and platinum(II) complexes. The platinum(II) complexes (**2** and **4**) were found to be less active against all cells. However, the palladium(II) complexes (**1** and **3**) show significant cytotoxicity on the sensitive cell lines. In particular, complex **3** exhibits a cytotoxicity, close to cisplatin and deserves further exploration *in vitro* and *in vivo* screening.

Acknowledgements

This work is a part of a research project 106T664. We thank TUBITAK for the financial support given to the project.

Appendix A. Supplementary data

CCDC 783745 and 783746 contain the supplementary crystallographic data for complexes **3** and **4**. These data can be obtained free of charge via http://www.ccdc.cam.ac.uk/conts/retrieving.html, or from the Cambridge Crystallographic Data Centre, 12 Union Road, Cambridge CB2 1EZ, UK; fax: (+44) 1223-336-033; or e-mail: deposit@ccdc.cam.ac.uk.

References

[1] B. Rosenberg, L. Van Camp, T. Krigas, Nature 205 (1965) 698.
[2] L.R. Kelland, N.P. Farrell, Platinum-Based Drugs in Cancer Therapy, Humana, Totowa, 2000.
[3] K.R. Harrap, Cancer Treat. Rev. 12 (1985) 21.
[4] Y. Kidani, K. Inagaki, J. Med. Chem. 21 (1978) 1315.
[5] L.M. Pasetto, R.M. D'Andrea, A.A. Brandes, E. Rossi, S. Monfardini, Crit. Rev. Oncol. Hematom. 60 (2006) 59.
[6] A. Garoufis, S.K. Hadjikakou, N. Hadjiliadis, Coord. Chem. Rev. 253 (2009) 1384.
[7] E.J. Baran, V.T. Yilmaz, Coord. Chem. Rev. 250 (2006) 1980.
[8] D.M. Roundhill, Inorg. Chem. 9 (1970) 254.
[9] W. Henderson, B.K. Nicholson, D.C. Chung, Acta Cryst. E58 (2002) m432.
[10] W. Henderson, B.K. Nicholson, L.J. McCaffrey, Inorg. Chim. Acta 285 (1999) 145.
[11] M. Cavicchioli, A.C. Massabni, E.E. Castellano, L.P.B. Sabeh, C.M. Costa-Neto, Inorg. Chim. Acta 360 (2007) 3055.
[12] N.S.C.R. Kumar, I.V.P. Raj, A. Sudalai, J. Mol. Catal. A: Chem. 269 (2007) 218.
[13] E. Guney, V.T. Yilmaz, A. Sengul, O. Buyukgungor, Inorg. Chim. Acta 363 (2010) 438.
[14] E. Guney, V.T. Yilmaz, C. Kazak, Polyhedron 29 (2010) 1285.
[15] E. Guney, V.T. Yilmaz, O. Buyukgungor, Inorg. Chim. Acta 363 (2010) 2416.
[16] V.T. Yilmaz, A. Ertem, E. Guney, O. Buyukgungor, Z. Anorg. Allg. Chem. 636 (2010) 610.
[17] E. Ulukaya, F. Ari, E. Guney, V.T. Yilmaz, in preparation.
[18] B. Pitteri, G. Marangoni, L. Cattalini, F. Visentin, V. Bertolasi, P. Gilli, Polyhedron 20 (2001) 869.
[19] G.M. Sheldrick, Acta Cryst. A64 (2008) 112.
[20] E. Ulukaya, F. Ozdikicioglu, A.Y. Oral, M. Demirci, Toxicol. In Vitro 22 (2008) 232.
[21] Z.D. Bugarcic, G. Liehr, R. van Eldik, J. Chem. Soc., Dalton Trans. (2002) 951.
[22] M.G.B. Drew, M.J. Riedl, J. Rodgers, J. Chem. Soc., Dalton Trans. 1 (1972) 234.
[23] Z.H. Zhang, X.H. Bu, Z.A. Zhu, Y.T. Chen, Polyhedron 15 (1996) 2787.
[24] A. Hazell, C.J. McKenzie, L.P. Nielsen, J. Chem. Soc., Dalton Trans. 1 (1998) 1751.
[25] Z. Nagy, I. Fabian, A. Benyei, Imre Sovago, J. Inorg. Biochem. 94 (2003) 291.
[26] S.I. Kirin, T. Wheyhermuller, K. Merz, N. Metzler-Nolte, Z. Anorg. Allg. Chem. 633 (2007) 2706.
[27] J. Tao, Z.J. Ma, R.B. Huang, L.S. Zhen, Inorg. Chem. 43 (2004) 6133.
[28] B. Pitteri, G. Annibale, G. Marangoni, V. Bertolasi, V. Ferretti, Polyhedron 21 (2002) 2283.
[29] W. Paw, S.D. Cummings, M.A. Mansour, W.B. Connick, D.K. Geiger, R. Eisenberg, Coord. Chem. Rev. 171 (1998) 125.
[30] R.C. Evans, P. Douglas, C.J. Winscom, Coord. Chem. Rev. 250 (2006) 2093.
[31] A.C.F. Caires, E.T. Almeida, A.E. Mauro, J.P. Hemerly, S.R. Valentini, Quim. Nova 22 (1999) 329.
[32] F.K. Keter, S. Kanyanda, S.S. Lyantagaye, J. Darkwa, D.J. Rees, M. Meyer, Cancer Chemother. Pharmacol. 63 (2008) 127.
[33] J. Kuduk-Jaworska, A. Puszko, M. Kubiak, M. Pelczynska, J. Inorg. Biochem. 98 (2004) 1447.